IL NUOVO CIMENTO Vol. 35 C, N. 6 Novembre-Dicembre 2012
DOI 10.1393/ncc/i2012-11366-6

Colloquia: LaThuile12

Heavy-flavor physics at the Tevatron

H. Miyake on behalf of the CDF and D0 Collaborations
High Energy Accelerator Research Organization - Tsukuba, Ibaraki, Japan

ricevuto il 7 Settembre 2012

Summary. — The CDF and D0 experiments at the Fermilab Tevatron proton-antiproton collider have been producing world's leading results on many interesting heavy-flavor physics topics. We report here three recent CDF results on B_s^0 meson dynamics. An updated search for ultra rare B_s^0 meson decays into dimuon final states and new bounds on the B_s^0 mixing phase and decay-width difference using $B_s^0 \to J/\psi\phi$ decays are summarized, both based on the whole Run II dataset corresponding to $10\,\mathrm{fb}^{-1}$. A new measurement of the branching fractions of the $B_s^0 \to D_s^{(*)+} D_s^{(*)-}$ decays uses $6.8\,\mathrm{fb}^{-1}$ of data is also reported.

PACS 11.30.Er – Charge conjugation, parity, time reversal, and other discrete symmetries.
PACS 13.20.He – Decays of bottom mesons.
PACS 13.25.Hw – Decays of bottom mesons.

1. – Introduction

Heavy-flavor physics enables probing the fundamental structure of matter and its interactions. Besides its significant contributions in establishing the standard model (SM), flavor physics plays a central role in the pursuit of new physics beyond the standard model (BSM). Decays of B_s^0 mesons are especially interesting since limited experimental information was available until recently, and a few tantalizing puzzles have emerged from data, *e.g.* the 3.9σ anomaly in the dimuon charge asymmetry [1].

In the last decade, the Tevatron $p\bar{p}$ collider at $\sqrt{s} = 1.96\,\mathrm{TeV}$ has been providing the most promising opportunity to study B_s^0 physics. At the Tevatron, b quarks are pair-produced with a cross section [2] three orders of magnitude higher than at e^+e^- colliders, and with an energy sufficient to generate all sorts of b hadrons. This allowed study of ultra rare decays, such as those arising from flavor changing neutral current (FCNC) processes and to first access measurements of CP-violating parameter in B_s^0 meson mixing and decay.

The Tevatron ended its operations in late September 2011, and many analyses are now in progress at CDF and D0 that use the whole dataset, corresponding to about

$10\,\mathrm{fb}^{-1}$ or a large fraction of that. We report here three recent CDF results including an updated search for rare B_s^0 meson decays, new bounds on the B_s^0 mixing phase and on the B_s^0 mass-eigenstates decay-width difference using $B_s^0 \to J/\psi\phi$ decays, and the measurement of the branching fractions of the $B_s^0 \to D_s^{(*)+} D_s^{(*)-}$ decays.

2. – $B_{s,d} \to \mu\mu$

The $B_s^0(B^0) \to \mu^+\mu^-$ decays involve a flavor-changing neutral current (FCNC) process. The decay rates are further suppressed by the helicity factor, $(m_\mu/m_B)^2$. The B^0 decay is also suppressed with respect to the B_s^0 decay by the ratio of CKM elements, $|V_{td}/V_{ts}|^2$. The SM expectations for these branching fractions are $\mathcal{B}(B_s^0 \to \mu^+\mu^-) = (3.2 \pm 0.2) \times 10^{-9}$ and $\mathcal{B}(B^0 \to \mu^+\mu^-) = (1.0 \pm 0.1) \times 10^{-10}$ [3]. As many new physics models can enhance the rate significantly, these decays provide sensitive probes for new physics. Over the last decade, ever improving upper limits where set by the CDF and D0 collaborations, which strongly constrained the parameters space of such models.

Using $7\,\mathrm{fb}^{-1}$ of data, in 2011 CDF reported an intriguing excess of signal-like events over background in the $B_s^0 \to \mu^+\mu^-$ channel at a level of 2.5 standard deviations, which led to the first double-sided bounds on the rate of the $B_s^0 \to \mu^+\mu^-$ [4]. Despite the hint of an excess, the CDF result was compatible with the SM expectation and null searches with similar sensitivity by LHCb [5] and CMS [6] as well as with an older D0 result [7]. In early 2012, CDF updated the analysis to the whole dataset of nearly $10\,\mathrm{fb}^{-1}$ to further investigate such effect. No improvements were introduced in the analysis on purpose to keep it identical to the $7\,\mathrm{fb}^{-1}$ analysis and study the evolution of the effect in the most unbiased way.

CDF selects two oppositely-charged muon candidates within a dimuon mass $4.669 < m_{\mu^+\mu^-} < 5.969\,\mathrm{GeV}/c^2$. The muon candidates are required to have $p_T > 2.0\,\mathrm{GeV}/c$, and $\vec{p_T}^{\mu^+\mu^-} > 4\,\mathrm{GeV}/c$, where $\vec{p_T}^{\mu^+\mu^-}$ is the transverse component of the sum of the muon momentum vectors. Data are divided into two exclusive categories, "CC" (both muon in the central detector) and "CF" (one muon central the other muon forward). The event selection is optimized using an artificial neural network (NN) that uses 14 discriminating variables, such as the dimuon isolation and dimuon impact parameter. The NN discriminant is designed to have no dimuon mass dependence, and such a condition is verified by cross checks data. Figure 1 shows both the signal and background distribution represented by the simulated signal and the sideband data.

The dominant residual background comes from the smoothly distributed combinatorial component. Peaking backgrounds from $B \to hh$ decays where the hadrons fake muons also contribute. Their effect is determined from data and simulation to affect the B_d^0 search more than the B_s^0. The background estimation is tested in various control samples, *e.g.* opposite-sign muon pairs which have negative B lifetime or same-sign dimuons, showing good agreement with observed background yields.

Data from the $B^0 \to \mu^+\mu^-$ search are shown in fig. 2. The data are consistent with the background prediction, yielding an observed limit of $\mathcal{B}(B^0 \to \mu^+\mu^-) < 4.6(3.8) \times 10^{-9}$ at the 95% (90%) CL An ensemble of background-only pseudoexperiments is used to estimate the consistency of data with the background-only hypothesis as a p-value of 41%. In the B_s^0 search, the data show a mild excees over background prediction in bins with NN > 0.97 (fig. 3) The p-value for the background-only hypothesis is 0.94%, which becomes 7.1% if the hypothesis of a SM signal and background is tested. A likelihood fit determines $\mathcal{B}(B_s^0 \to \mu^+\mu^-) = (1.3^{+0.9}_{-0.7}) \times 10^{-8}$. Additionally, a bound at 90% (95%) CL

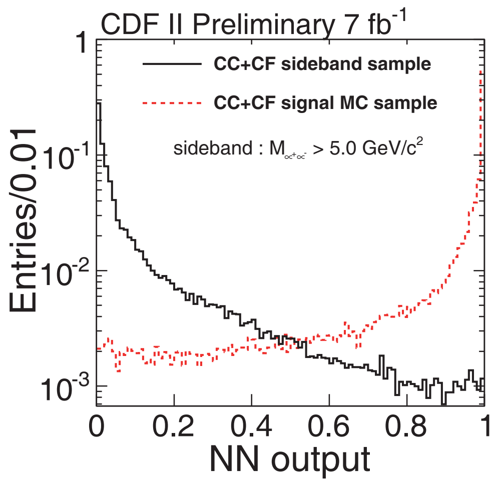

Fig. 1. – NN distributions of the simulated signal (dashed) and the sideband data (solid).

on the branching fraction of the $B_s^0 \to \mu^+\mu^-$ is set at $0.8 \times 10^{-9} < \mathcal{B}(B_s^0 \to \mu^+\mu^-) < 3.9 \times 10^{-8}$ ($2.2 \times 10^{-9} < \mathcal{B}(B_s^0 \to \mu^+\mu^-) < 3.0 \times 10^{-8}$). The mild excess observed in summer 2011 is not reinforced by the 30% additional data, but a larger than 2σ deviation from the background-only expectation remains. These results are consistent with previous CDF measurement [4], other experiments [7-9], and the SM.

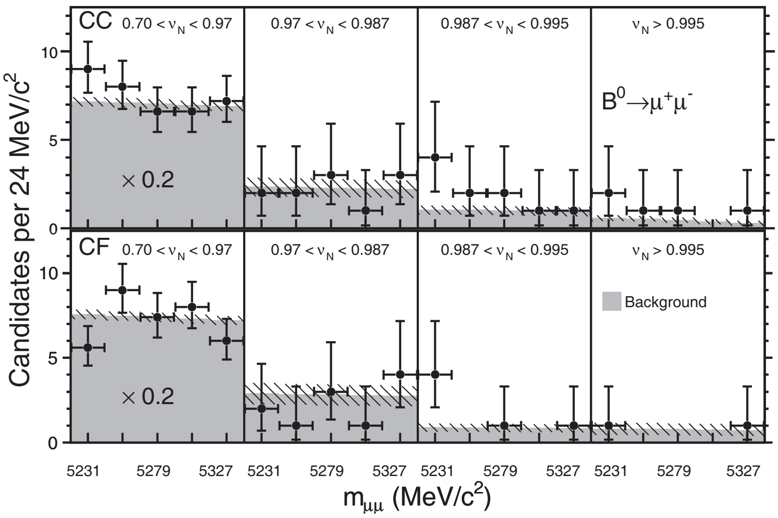

Fig. 2. – Dimuon mass distributions for the $B^0 \to \mu^+\mu^-$ measurements. The CC (top) and CF (bottom) categories are divided into 8 NN bins each, of which the lowest 5 NN bins are combined into one bin. The data points represent the observed number of events. The solid (hashed) areas show the background estimates (their systematic uncertainties).

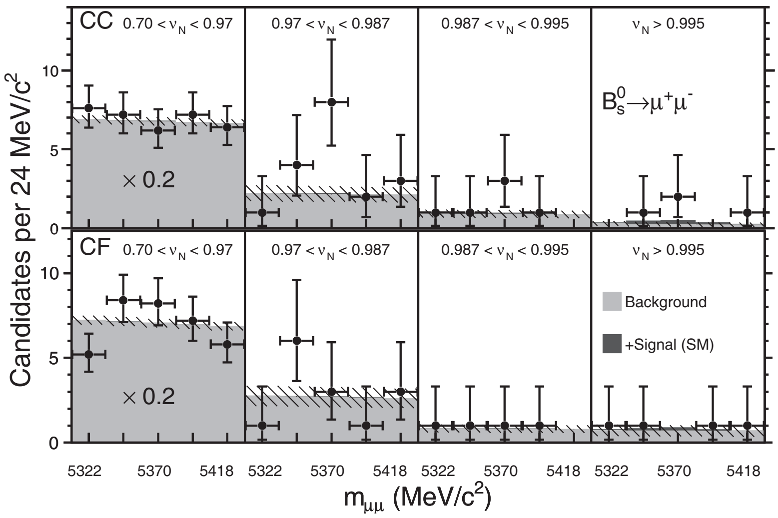

Fig. 3. – Dimuon mass distribution for the $B_s^0 \to \mu^+\mu^-$ measurements. The SM expectations are shown by the dark-gray areas, as in fig. 2.

3. – *CP* violation in the B_s^0 system

As in the neutral B^0 system, *CP* violation in the B_s^0 system may occur also through interference of decays with and without the B_s^0-$\overline{B}_s^0$ mixing. The B_s^0-$\overline{B}_s^0$ mixing occurs via second-order weak processes. It is described in the SM by Δm_s and $\Delta\Gamma_s$, the mass and decay width difference of the two mass eigenstates, $B_{s\,H}^0$ and $B_{s\,L}^0$. The quantity $\Delta\Gamma_s = \Gamma_{sL} - \Gamma_{sH} = 2|\Gamma_{12}|\cos(\phi_s)$ is sensitive to new physics effects that affect the phase $\phi_s = \arg(-M_{12}/\Gamma_{12})$, where Γ_{12} and M_{12} are the off-diagonal elements of the mass and decay matrices and $\Gamma_{sH}(\Gamma_{sL})$ is the decay width of $B_{s\,H}^0$ ($B_{s\,L}^0$). In the SM, the B_s^0-$\overline{B}_s^0$ *CP*-violating phase $\phi_s^{\rm SM}$ is predicted to be as small as 0.004 [10]. However a broad class of BSM models predict new sources of *CP* violation that can greatly enhance it. If such new physics has a different phase $\phi_s^{\rm NP}$ from the SM, the ϕ_s could be dominated by $\phi_s^{\rm NP}$. The most promising probe of the phase is the study of the time-evolution of $B_s^0 \to J/\psi\phi$ decays, where the *CP*-violating phase $\beta_s^{J/\psi\phi}$ enters. This is defined as the phase between the direct $B_s^0 \to J/\psi\phi$ decay amplitude and mixing followed by decay amplitude. The phase $\beta_s^{\rm SM}$ is described by CKM matrix elements as $\arg(-V_{ts}V_{tb}^*/V_{cs}V_{cb}^*)$ and predicted to be small, 0.02 [10]. Since $\phi_s^{\rm NP}$ contributes to both ϕ_s and β_s, large β_s would indicate the existence of a new physics contribution. CDF updates the β_s measurement using the whole dataset, collected with a low-p_T dimuon trigger corresponding to nearly $10\,{\rm fb}^{-1}$. Candidate $B_s^0 \to J/\psi\phi$ decays are reconstructed from $J/\psi \to \mu^+\mu^-$ and $\phi \to K^+K^-$ final states. About 11 000 signal events are selected with a neural network discriminator (fig. 4 (left)). To extract $\Delta\Gamma_s$ and β_s, an unbinned maximum-likelihood fit is performed on the time-evolution of signal candidates. Enhanced sensitivity to the desired observables is reached by using an angular analysis to statistically separate *CP*-even and -odd final states. Information about mixing is obtained from tagging the production flavor of the bottom-strange mesons. Two flavor tagging algorithms are employed, opposite-side tagging (OST) and same-side kaon

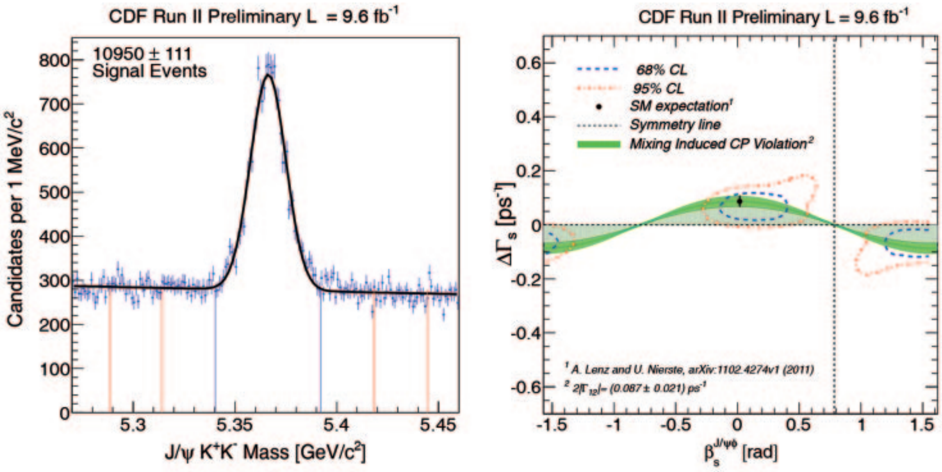

Fig. 4. – Left: $J/\psi K^+K^-$ mass distribution. Right: Two-dimensional 68% (95%) C.L. regions of $\beta_s^{J/\psi\phi}$ (horizontal) and $\Delta\Gamma_s$ (vertical) shown as enclosed by the dashed (dot-dashed) contours. The shaded band shows the allowed region if only mixing-induced *CP* violation occurs.

tagging (SSKT). The OST exploits the charge information of decay products coming from opposite side of the B_s^0 meson while the SSKT uses the charge of the kaon produced in association with the b or $\bar{b}$ quark in the fragmentation process. OST has been recalibrated using about 82 000 $B^\pm \to J/\psi K^\pm$ decays, achieving a tagging performance of $\varepsilon D^2 = (1.39 \pm 0.01)\%$. The SSKT algorithm has only been used in half of the data sample ($\varepsilon D^2 = (3.2 \pm 1.4)\%$), since calibration on the full sample has not been completed yet. This degrades the statistical resolution of the mixing phase measurement by no more than 15%. Assuming no *CP* violation, CDF finds

$$
\begin{aligned}
\tau_s &= 1.528 \pm 0.019(\text{stat}) \pm 0.009(\text{syst})\,\text{ps},\\
\Delta\Gamma_s &= 0.068 \pm 0.026(\text{stat}) \pm 0.007(\text{syst})\,\text{ps}^{-1},\\
|A_0(0)|^2 &= 0.512 \pm 0.012(\text{stat}) \pm 0.017(\text{syst}),\\
|A_{||}(0)|^2 &= 0.229 \pm 0.010(\text{stat}) \pm 0.014(\text{syst}),\\
\delta_\perp &= 2.79 \pm 0.53(\text{stat}) \pm 0.15(\text{syst})\,\text{rad}.
\end{aligned}
$$

These quantities are consistent with previous measurements [11, 12] and amongst the world's most precise currently available. From a fit in which *CP* violation is allowed, CDF extracts confidence intervals using a profile-likelihood ratio statistics in which coverage has been verified against the effect of systematic uncertainties and irregularities of the likelihood, $\beta_s \in [-\pi/2, -1.51] \cup [-0.06, 0.30] \cup [1.26, \pi/2]$ at the 68% confidence level, and $\beta_s \in [-\pi/2, -1.36] \cup [-0.21, 0.53] \cup [1.04, \pi/2]$ at the 95% confidence level, in agreement with the SM prediction. CDF also reports 68% and 95% confidence regions in the β_s-$\Delta\Gamma_s$ plane including systematic uncertainties in fig. 4 (right). The measurements are compatible with the SM predictions of β_s and $\Delta\Gamma_s$ within less than one standard deviation, and also consistent with other recent determinations [12, 13].

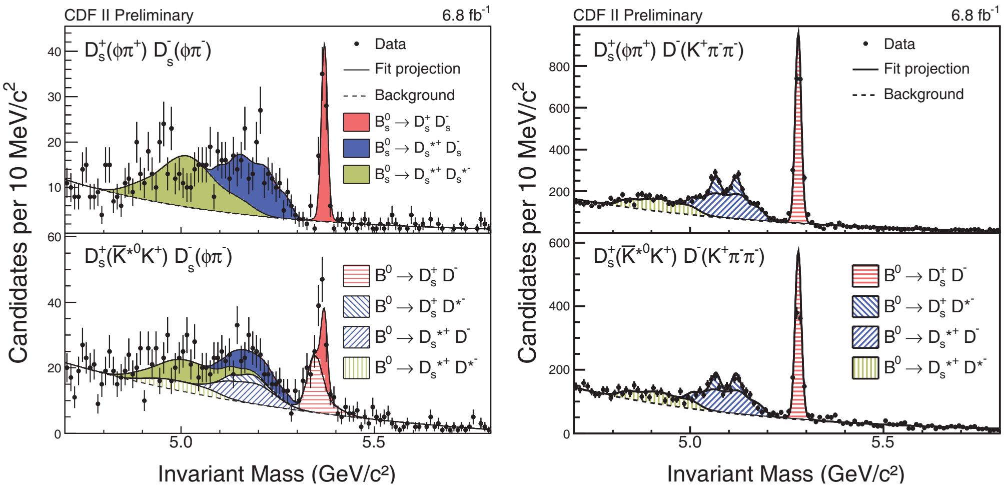

Fig. 5. – From top-left to bottom-right, $B_s^0 \to D_s^+(\to \phi\pi^+)D_s^-(\to \phi\pi^-)$, $B^0 \to D_s^+(\to \phi\pi^+)D^-(\to K^+\pi^-\pi^-)$, $B_s^0 \to D_s^+(\to \bar{K}^{*0}K^+)D_s^-(\to \phi\pi^-)$, $B^0 \to D_s^+(\to \bar{K}^{*0}K^+)D^-(\to K^+\pi^-\pi^-)$ invariant mass distributions, respectively. The points show data. The solid curves and dashed curve mean the fitted signals and background, respectively.

4. – $B_s^0 \to D_s^{(*)+}D_s^{(*)-}$

A measurement of the decay rates of $B_s^0 \to D_s^{(*)+}D_s^{(*)-}$ decays may provide useful information on the B_s^0 width difference in the SM. Some authors suggest that $\Delta\Gamma_s/\Gamma_s$ can be inferred by a measurement of $\mathcal{B}(B_s^0 \to D_s^{(*)+}D_s^{(*)-})$ under certain theoretical assumptions on the decay model [14, 15], *i.e.*,

$$(1) \qquad 2\mathcal{B}(B_s^0 \to D_s^{(*)+}D_s^{(*)-}) \sim \frac{\Delta\Gamma_s}{\Gamma_s + \Delta\Gamma_s/2}\,.$$

However, it has been pointed out recently that three-body decays may provide a significant contribution to $\Delta\Gamma_s$, thus invalidating the above relationship. The branching fractions have been measured by CDF [16], D0 [17], and Belle [18], but more data are necessary to reach a precision that can provide some constraint on $\Delta\Gamma_s$.

CDF updates the measurement of the decay modes using $6.8\,\text{fb}^{-1}$ of data collected with a trigger on tracks displaced by the primary $p\bar{p}$ interaction. The decays are partially reconstructed as $B_s^0 \to D_s^+D_s^- +$ anything, since the photon and the neutral pion from the $D_s^{*+} \to D_s^+\gamma$ and $D_s^{*+} \to D_s^+\pi^0$ decays are not reconstructed due to their low detection efficiency. The D_s meson is reconstructed from $D_s \to K^{*0}K$ or $D_s \to \phi(\to KK)\pi$ decays. The K^{*0} meson is selected with $0.837 < M(K^-\pi^+) < 0.947\,\text{GeV}/c^2$ centered on the known K^{*0} mass and the ϕ meson is selected with $1.005 < M(K^+K^-) < 1.035\,\text{GeV}/c^2$ centered on the known ϕ mass. As a normalization channel, $B^0 \to D^+(\to K\pi\pi)D_s^-$ is reconstructed to normalize the branching fractions. Pairs of $D_s^+ \to \phi\pi^+$ or $D_s^+ \to \bar{K}^{*0}K^+$ candidates and $D_s^- \to \phi\pi^-$ candidates are combined to form B_s^0 candidates and fitted to a common vertex. Combinations of K^{*0} decay channels are not used since that final state has a large background compared to the signal. The event selection is further optimized using a neural network. A simultaneous fit to the reconstructed signal and normalization mass distribution yields B_s^0 production rate times $B_s^0 \to D_s^{(*)+}D_s^{(*)-}$

branching fractions relative to $B^0 \to D_s^+ D^-$:

$$f_X = \frac{f_s}{f_d} \frac{\mathcal{B}(B_s^0 \to X)}{\mathcal{B}(B^0 \to D_s^+ D^-)}\,, \tag{2}$$

for $X = D_s^+ D_s^-$, $D_s^{*\pm} D_s^{\mp}$, $D_s^{*+} D_s^{*-}$, and $D_s^{(*)+} D_s^{(*)-}$, where f_s/f_d is the relative production rate of B_s^0 to B^0 mesons. The simultaneous fit helps the determination of the yields of the four final states while properly accounting for the effect ofcross feeds. Figure 5 shows mass distributions with fit results overlaid. The D_s Dalitz structure is explicitly considered in the reconstruction for accurate acceptance determination and reduction of the relevant systematic uncertainty. The following absolute branching fractions are derived:

$$\begin{aligned}
\mathcal{B}(B_s^0 \to D_s^+ D_s^-) &= (0.49 \pm 0.06 \pm 0.05 \pm 0.08)\%,\\
\mathcal{B}(B_s^0 \to D_s^{*\pm} D_s^{\mp}) &= (1.13 \pm 0.12 \pm 0.19 \pm 0.09)\%,\\
\mathcal{B}(B_s^0 \to D_s^{*+} D_s^{*-}) &= (1.75 \pm 0.19 \pm 0.17 \pm 0.29)\%,\\
\mathcal{B}(B_s^0 \to D_s^{(*)+} D_s^{(*)-}) &= (3.38 \pm 0.25 \pm 0.30 \pm 0.56)\%.
\end{aligned}$$

The first, second, and third component of the uncertainty refers to the statistical, systematic, and normalization uncertainties, respectively. The above results are the most precise branching fractions for these modes from a single experiment.

REFERENCES

[1] Abazov V. M. *et al.* (D0 Collaboration), *Phys. Rev. D*, **84** (2011) 052007, arXiv:1106.6308.
[2] Aaltonen T. *et al.* (CDF Collaboration), *Phys. Rev. D*, **79** (2009) 092003, arXiv:0903.2403.
[3] Buras A. J. *et al.*, *JHEP*, **09** (2010) 106, arXiv:1002.2126.
[4] Aaltonen T. *et al.* (CDF Collaboration), *Phys. Rev. Lett.*, **107** (2011) 239903, arXiv:1107.2304.
[5] Aaij R. *et al.* (LHCb Collaboration), *Phys. Lett. B*, **708** (2012) 55.
[6] Chatrchyan S. *et al.* (CMS Collaboration), *Phys. Rev. Lett.*, **107** (2011) 191802, arXiv:1107.5834.
[7] Abazov V. M. *et al.* (D0 Collaboration), *Phys. Lett. B*, **693** (2010) 539, arXiv:1006.3469.
[8] Aaij R. *et al.* (LHCb Collaboration), arXiv:1203.4493 (2012).
[9] Chatrchyan S. *et al.* (CMS Collaboration), *JHEP*, **04** (2012) 033, arXiv:1203.3976.
[10] Lenz A. and Nierste U., *JHEP*, **06** (2007) 072, arXiv:hep-ph/0612167.
[11] Aaltonen T. *et al.* (CDF Collaboration), *Phys. Rev. D*, **85** (2012) 072002, arXiv:1112.1726.
[12] Abazov V. M. *et al.* (D0 Collaboration), *Phys. Rev. D*, **85** (2012) 032006, arXiv:1109.3166.
[13] LHCb Collaboration, LHCb-CONF-2012-002.
[14] Aleksan R., Le Yaouanc A., Oliver L., Pene O. and Raynal J., *Phys. Lett. B*, **316** (1993) 567.
[15] Dunietz I., Fleisher R. and Nierste U., *Phys. Rev. D*, **63** (2001) 114015, arXiv:hep-ph/0012219.
[16] Aaltonen T. *et al.* (CDF Collaboration), *Phys. Rev. Lett.*, **100** (2008) 021803.
[17] Abazov V. *et al.* (D0 Collaboration), *Phys. Rev. Lett.*, **102** (2009) 091801, arXiv:0811.2173.
[18] Esen S., arXiv:1110.2099 (2011).